

Cytoskeletal Injury and Subsarcolemmal Bleb Formation in Dog Heart During In Vitro Total Ischemia

MARTIN D. SAGE, MB ChB, PhD, and
ROBERT B. JENNINGS, MD

From the Department of Pathology, Duke University Medical Center, Durham, North Carolina

In previous studies a two-step hypothesis explaining the mechanism of lethal ischemic injury to cardiac myocytes has been advanced. It proposes that damage to the myocyte cytoskeleton precedes, and predisposes the cell to, mechanical injury induced by cell swelling or by ischemic contracture. This study quantitated the prevalence of breakage of the major cytoskeletal attachment between the plasmalemma and peripheral myofibers as a function of the duration (0–180 minutes) of *in vitro* total ischemia in dog heart papillary muscle. Breakages of Z-band, plasmalemmal attachment complexes were few before 120 minutes of ischemia, but thereafter became more prevalent; the transition between the initial rate of appearance of the

breaks and the later fast rates coincided with the appearance of severe cell swelling, ischemic contracture, and ultrastructural criteria of irreversible ischemic injury. Z-band, plasmalemmal attachment complex breakage and cell swelling resulted in formation of subsarcolemmal blebs. Two major bleb types have been discerned on ultrastructural appearance using as the criteria the preservation of integrity of the plasmalemma and subplasmalemmal leptomeres. The identification of two types of blebs suggests two independent mechanisms of injury, the first directed at Z-band attachments, and the second at the cytoskeletal structures of A- and I-band regions of the plasmalemma. (Am J Pathol 1988, 133:327–337)

WHEN CARDIAC MUSCLE is deprived of coronary arterial flow *in vivo*, anaerobic metabolism supervenes and high energy phosphate compounds are degraded with formation of multiple smaller molecular species, chiefly lactate, creatine, and inorganic phosphate.¹ The resulting rise in sarcoplasmic osmolarity^{2,3} is associated with entry of water from the extracellular space; this cell swelling is manifested morphologically as an increase in the size and electron lucency of the sarcoplasm. Such swelling can be modeled and experimentally manipulated *in vitro* by incubation of slices of heart muscle in hypotonic media⁴ or by perfusion of isolated beating hearts *in vitro* with hypotonic solutions.⁵ In either model, heart muscle cells are capable of tolerating considerable hypo-osmotic stress while adequately oxygenated, but under anoxic conditions, lethal cell injury occurs: there is severe cell swelling resulting in blebbing of the sarcolemma and plasmalemmal disruption. Sarcolemma is defined as the plasmalemma and surface lamina together.

To explain this effect of anoxia, authors^{4,5} have suggested a two-step mechanism. Anoxia first causes an

as yet undefined injury to the plasmalemma or its supporting structures, and then the osmotically-induced distensive stress of cell swelling, even though well tolerated by normoxic cells, mechanically disrupts the cell, leading directly to plasmalemmal disruption and cell death. Both groups have presented evidence^{6,7} that the first phase injury may be damage to the myocyte cytoskeleton, particularly to the attachment complexes formed between myofibrillar Z-bands and the plasmalemma.

The degree of cell swelling seen in isolated crystalloid perfused hearts or incubated slices of myocardium may be excessive compared with that which would occur *in vivo*. A relative excess of water is available to cells in these “continuous flow” models be-

Supported in part by NIH grants HL23138 and HL27416. Dr Sage was a Medical Research Council of New Zealand Overseas Research Fellow at the time of this study. Accepted for publication June 21, 1988.

Address reprint requests to Robert B. Jennings, MD, Department of Pathology, Box 3712, Duke University Medical Center, Durham, NC 27710.

cause both use crystalloid perfusate or incubating solutions without oncotic pressor agents,⁸ and both methods make virtually infinite extracellular water available to anoxic cells. Neither of these situations may accurately represent that of myocardium *in vivo* deprived completely of its blood supply, and beyond diffusion distance from adjacent normoxic muscle.

This study has used the well-documented model of *in vitro* total ischemia,^{9,10} which ensured uniform severe ischemia, reduced the proportion of cells physically disrupted during dissection of samples compared with incubated thin slices, and did not present incubated cells with excessive exogenous water. *In vitro* total ischemia nonetheless induced severe cell swelling, including the formation of subsarcolemmal blebs. The structure of the subsarcolemmal blebs, and the prevalence of breakage of Z-band/plasmalemmal attachment complexes (Z/PACs) that leads to their formation, were investigated with transmission electron microscopy of ultrathin sections and deep-etch rotary-coated platinum-carbon replicas, and with scanning electron microscopy. Three types of blebs were discriminated on the basis of their appearance; the key feature in this classification was the detachment and loss from the plasmalemma of the microfibrillar array known as leptomeres, structures whose role in cardiac muscle cells has been indicated¹¹ to probably be cytoskeletal.

Methods

Tissue Sampling

Four healthy mongrel dogs of either sex were anesthetized with pentobarbital and their hearts rapidly excised through a left fourth intercostal incision. The left ventricle was layed open and anterior or posterior papillary muscles excised from the free wall. The myotendinous tip was excised and discarded. A small sample of the papillary muscle was diced immediately into 1-mm cubes and placed in fixative to serve as a control (0 minutes ischemia). The remainder was wrapped in moistened (0.9% NaCl) gauze, placed in a resealable polythene bag from which air was excluded, and incubated submerged in a shaking water bath at 37 C. At 30-minute intervals (30–180 minutes) the bag was removed from the bath and further samples were excised from the papillary muscle. Each new sample was trimmed at least 1 mm on all exposed edges, to exclude tissue affected by exogenous oxygen (room air) or water (gauze moisture), and then diced in fixative.

All tissue was fixed in freshly prepared 2% glutaraldehyde with 0.05 M lysine-HCl in 0.1 M cacodylate buffer at 37 C for 2 hours, followed by 22 hours in 4% glutaraldehyde at 4 C, and stored in buffer at 4 C.^{11,12}

Transmission Electron Microscopy

Fixed blocks were poststained in 1% OsO₄ in s-collidine buffer (30 minutes at 4 C), and 4% uranyl acetate in barbital-acetate buffer (10 minutes at 22 C), then dehydrated in a series of ethanols and propylene oxide before embedding in Epon. Blocks showing predominantly longitudinal orientation of myocytes were selected from toluidine-blue stained thick sections, trimmed, and ultra-thin sectioned, then stained with uranyl acetate and lead citrate before examination at 60–80 kV in JEOL JEM100B or Hitachi HU-11E microscopes.

Scanning Electron Microscopy

Fixed tissue blocks were processed as described previously.¹³ Briefly, the tannic acid/osmium/thiocarbohydrazine/osmium postfixation sequence was used before ethanol dehydration and freeze-cleavage under liquid nitrogen. Thawed fragments were critical point dried from carbon dioxide, mounted on aluminum stubs with conductive paint, and coated thinly with gold-palladium in a sputter coater. Samples were viewed in a JEOL JSM35C scanning electron microscope at 20–30 kV accelerating voltage.

Platinum-Carbon Rotary Replicas

The methods of Isobe and Shimada¹⁴ and Nassar *et al*¹⁵ were combined and modified. Fixed tissue blocks were postfixated in 2% tannic acid (30 minutes) and 1% OsO₄ (2 hours at 4 C), then dehydrated in a series of ethanols up to 70%. Aluminium disks were prepared by gluing polyethylene filter paper disks to their surface with Araldite,¹⁵ and the specimen mounted on the paper disk with a small drop of 20% aqueous gelatin before plunging the disk into liquid nitrogen. Disk and sample were transferred to the precooled stage of a Balzer BAF301 freeze-fracture device, a fracture plane microtomed at 174.5 K and the surface etched at that temperature for 90 minutes at a pressure of less than 2×10^{-6} mmHg. The face was shadowed with platinum (12–25° shadow angle) and carbon (90°) while the specimen was rotated at 40–60g. After vacuum release the fracture face was coated with collodion (1% in amyl acetate, Ernest Fullam Co., Latham, NY), and the tissue digested from the replica by domestic hypochlorite bleach. Cleaned replicas were rinsed in distilled water, picked up on formvar-coated grids, and air-dried. Collodion was removed by wafting the grid through fresh amyl acetate. Replicas were viewed in a JEOL JEM100B transmission electron microscope at 60–80 kV and printed in photographically reversed contrast.

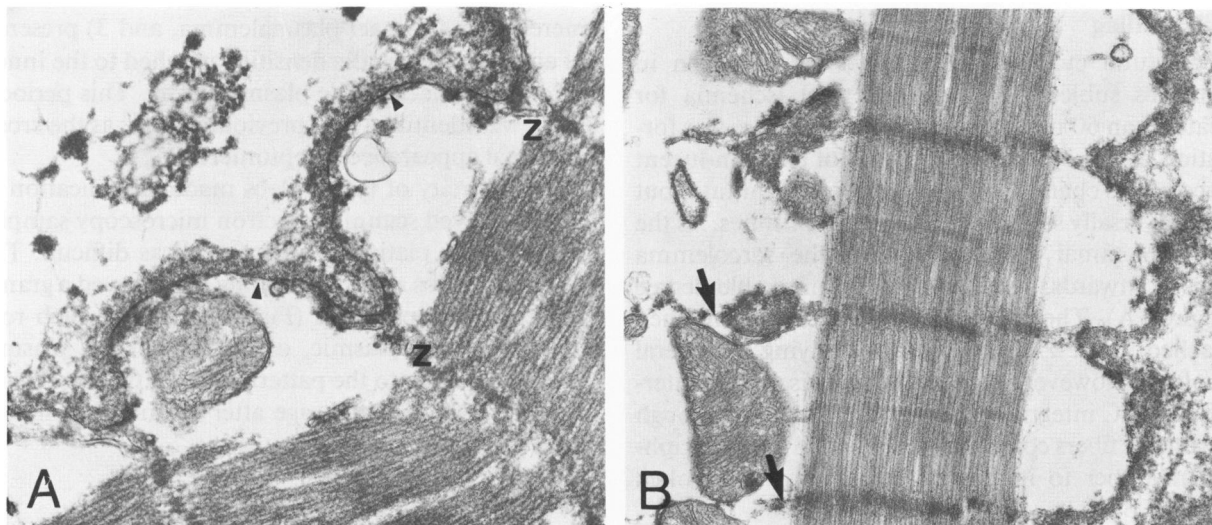


Figure 1—Transmission electron micrographs of dog papillary muscle after 150 minutes *in vitro* total ischemia showing: **A**—marked distensive bulging of the sarcolemma (arrow heads) but intact Z-band/plasmalemmal attachment complexes (z) ($\times 27,500$); and **B**—fragments of disrupted anchor fibers (arrows) between a peripheral myofiber and its deeper neighbours ($\times 16,300$).

Quantitation of Z-band/Plasmalemmal Attachment Complex Breakage

Two grids, each with at least three sections, were cut from each of two blocks for these samples: 0, 30, 60, 90, 120, 150, and 180 minutes of *in vitro* total ischemia. Such a set (28 grids) was prepared for each incubated papillary muscle. From each grid, 25 areas showing myocyte sarcolemma were selected by electron microscopic examination according to these criteria: 1) each area contained five contiguous sarcomeres all sectioned longitudinally so that all six Z/PACs could be seen without interruption or obliquity; 2) no more than one area was selected from each side of a sectioned myocyte or two in total per cell; 3) areas were located by finding the central grid square of a region of longitudinally orientated myocytes, photographing all suitable areas in that square, then traversing to the next grid square in a clockwise spiral pattern. Typically three-four grid squares (300 mesh) were used to find 25 suitable areas.

Each of the 150 Z/PACs in each set of 25 areas was classed as either “intact” (showing structural attachment or proximity of less than 100nm between Z-band and plasmalemma) or “broken.” Mean values of number “intact” per set of 150 Z/PACs, and standard errors of the means, were determined for each papillary muscle series, and also for pooled samples at each ischemic interval. Differences between means was tested by one-way analysis of variance, recognising a probability of 1% or less as significant.

Results

This section describes several features of dog papillary muscle subjected to *in vitro* total ischemia, in-

cluding cell swelling and cytoskeletal disruption within myocytes; quantitation of the breakage of the major peripheral cytoskeletal structure—the Z/PAC; and the ultrastructural appearance of the three types of subsarcolemmal blebs which result from cell swelling and cytoskeletal failure.

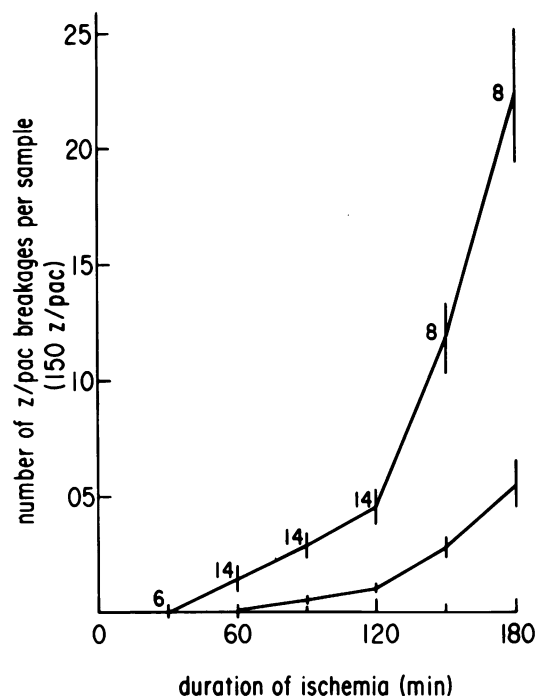


Figure 2—A graph showing the prevalence of myofibrillar Z-band plasmalemmal attachment complex breakage (upper line), and subsarcolemmal bleb prevalence (lower line), as a function of increasing duration of *in vitro* total ischemia. The number of samples (each of 150 Z/PACs) is given for each mean; the bars are standard errors.

Cell Swelling

Structural evidence of cell swelling was seen in myocytes subjected to *in vitro* total ischemia for greater than 60 minutes: within the cell there was formation and progressive expansion of electron-lucent spaces. This change was mild before 120 minutes but was universally severe at 150 and 180 minutes. As the subsarcolemmal space expanded, the sarcolemma bulged outwards, sometimes to a remarkable degree (Figure 1A). The plasmalemma generally remained attached to the Z-band of the underlying peripheral myofibril, however, even at the later ischemic intervals. Z/PAC integrity was often retained even though the anchor fibers connecting the Z-band of the peripheral myofiber to its deeper neighbors were broken (Figure 1B).

Quantitation

The increase in prevalence of Z/PAC breakage with prolongation of the ischemic insult is shown in Figure 2. Note that broken Z/PACs were virtually absent before 60 minutes, and that the rate of increase in prevalence between 60 and 120 minutes is small: the mean value at 120 minutes (4.50 ± 0.71) still only represents 3% of Z/PACs. After 120 minutes, however, the rate of increase was marked and the proportion of Z/PAC breakages reached 14.4% (22.12 ± 2.84) by 180 minutes. Differences between 60 and 120 minutes and between 120 and 180 minutes were statistically significant.

Blebs were defined as consisting of areas with two or more *adjacent* Z/PACs showing breakage, and the prevalence of blebs (lower line Figure 2) showed a biphasic rate of increase that was similar to that seen for Z/PAC breakages alone. No blebs of any type were present before 60 minutes, and at that time only a single bleb was seen. By 90 minutes blebs were reliably present and by 120 minutes averaged one bleb per 150 Z/PAC sample. The transition point in the rate of increase was at 120 minutes, just as it was for the onset of severe cell swelling and Z/PAC breakage. This was also the time at which high amplitude mitochondrial swelling, amorphous densities in mitochondrial matrix, and plasmalemmal defects were first seen: ultrastructural criteria of irreversible ischemic injury.

Type I Blebs

The first type of bleb noted during the progress of ischemic injury was termed type I. These blebs were the only type seen before 120 minutes, but were also frequently observed in modified form at later time intervals. The appearance of Type I blebs is illustrated in Figures 3–5; their key features were 1) Z/PAC breakage to form a space usually three to five sarco-

meres long, 2) intact plasmalemma, and 3) presence of an array of periodic densities attached to the inner, cytoplasmic face of the plasmalemma. This periodic array was identified by a previous study¹¹ as the cross-sectional appearance of leptomeres.

The scarcity of type I blebs made identification in freeze-cleaved scanning electron microscopy samples or deep-etch platinum-carbon replicas difficult. The few type I blebs seen by scanning EM showed a granular-nodular appearance (Figure 5) on the bleb roof (the inner, cytoplasmic, or PS face of the plasmalemma), similar to the pattern seen on that face when exposed by freeze-cleavage after 40 minutes *in vivo* ischemia.¹³

Type II Blebs

Type II blebs were first seen at 120 minutes and became increasingly common, until by 180 minutes, the type II form was predominant. They were easily distinguished from type I blebs that, after 120 minutes of *in vitro* total ischemia, retained their appearance except for increasingly common plasmalemmal defects. Type II blebs (Figures 6–8) typically contained an organelle-free space, and differed from type I blebs at both base and roof. The roof contained plasmalemma that showed defects of such size and frequency as to make them 1) a constant feature, and 2) highly unlikely to be the result of plane of section or fixation artefact. In some areas of the roof there was separation from the plasmalemma of the surface lamina, and in virtually all areas there was separation from the plasmalemma of the leptomere arrays that characterise type I blebs and ischemic sarcomeres without blebs. The bleb base showed a new feature: a densely staining fibrillar mat adherent to Z/PACs and extending the length of the sarcomere, appearing to bind peripheral mitochondria to the bleb floor. The authors have described this mat previously in sarcomeres that do not show blebs,¹¹ and have interpreted it as the degraded form of leptomeres, possibly incorporating other subplasmalemmal structures.

Type II blebs were frequently identified in scanning electron microscopy samples of myocardium ischemic for more than 120 minutes. They differed from type I blebs in showing a smooth, almost featureless inner surface to the roof (Figure 9A), and on the bleb floor, a complex of adherent material (Figure 9B). This coarse array was dissimilar to the features of normal or ischemic peripheral myofibers exposed by fortuitous freeze-cleavage planes.

Deep-etch replica preparations of control and early ischemic (up to 90 minutes) samples could be reliably produced by the method described (Figures 10A, B). Replicas up to 1 mm wide could be obtained intact.

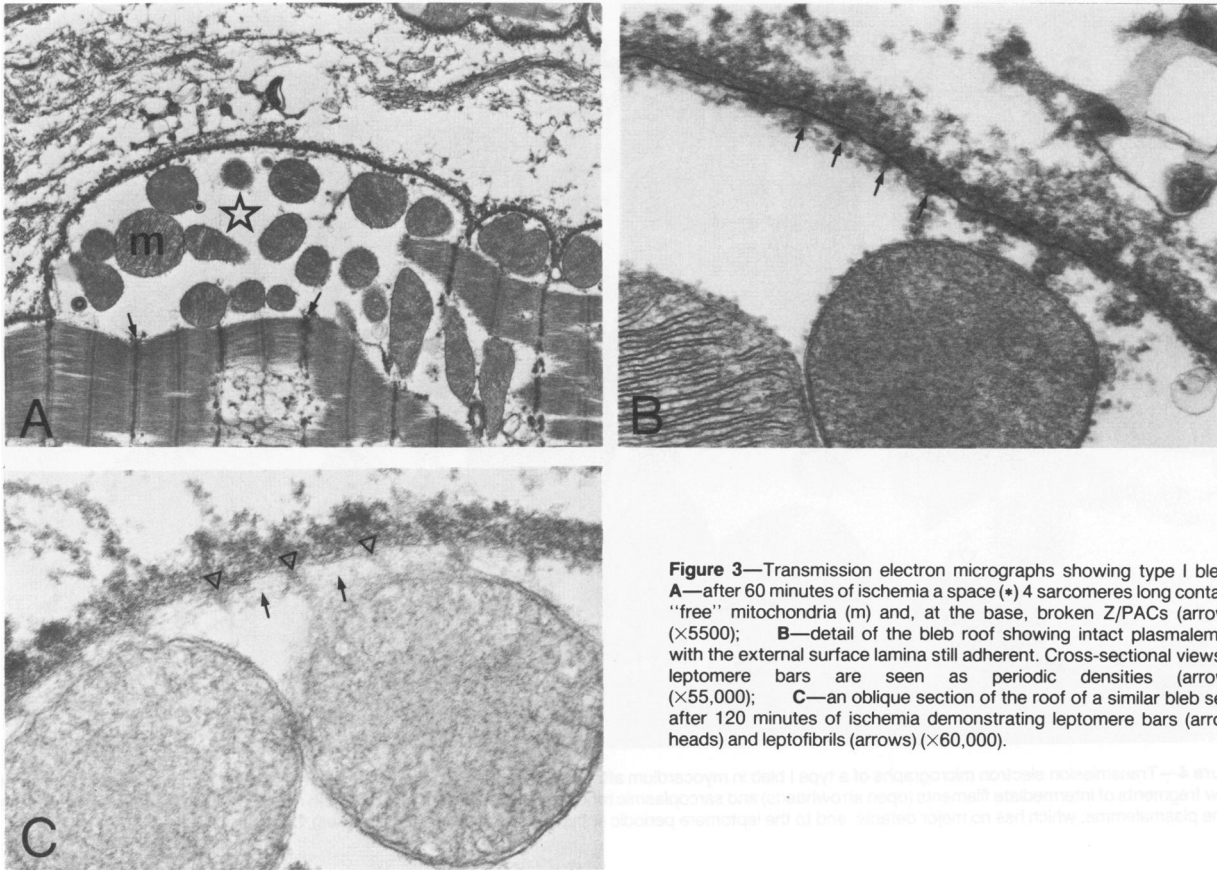


Figure 3—Transmission electron micrographs showing type I blebs: **A**—after 60 minutes of ischemia a space (*) 4 sarcomeres long contains "free" mitochondria (m) and, at the base, broken Z/PACs (arrows) ($\times 5500$); **B**—detail of the bleb roof showing intact plasmalemma with the external surface lamina still adherent. Cross-sectional views of leptomere bars are seen as periodic densities (arrows) ($\times 55,000$); **C**—an oblique section of the roof of a similar bleb seen after 120 minutes of ischemia demonstrating leptomere bars (arrowheads) and leptofibrils (arrows) ($\times 60,000$).

From ischemic samples taken 120 minutes and later, intact replicas could be obtained only rarely, most of them disintegrating during removal of the collodion backing. Occasional type II blebs were obtained, and Figure 10C shows an area where the surface lamina has separated from the plasmalemma and peripheral myofiber, and the Z/PACs (and probably plasmalemma) have been converted to foci of debris.

Type III Blebs

The third type of bleb noted may not be related to myocytes at all, but needs to be included in this account because of structural analogy. Type III blebs occurred *outside* myocytes in the extra-cellular space and were composed of organelle-free spaces bounded by tri-laminar membrane (Figures 11A, B). No Type III bleb showed recognizable surface lamina or leptomere components on its membrane, nor was continuity with myocyte plasmalemma demonstrated. On rare occasions, similar membrane-bound inclusions were present within type II bleb spaces, but virtually all type III blebs were in the interstitium with intimate relationship to capillaries. These features clearly discriminate type III blebs from types I and II; they have

not been included in the quantitative values above, and because they have been previously observed¹⁶ they are not discussed further.

Discussion

The data presented show that cytoskeletal injury, evident as breakage of Z/PACs and formation of subsarcolemmal blebs, occurred during total *in vitro* ischemia without the large exogenous water source inherent in models using cell-free crystalloid solutions as perfusates. By quantitating the increasing prevalence of individual Z/PAC breakages, it has been shown that in the present model most Z/PAC breakages and blebs appeared at, or after, the onset of irreversible ischemic injury. A relatively small number of ultrastructurally different blebs were seen before the time when most cells showed ultrastructural criteria of lethal injury, however. The existence of this subgroup, and the differences in structure between it and the more common and later-onset Type II blebs, suggests that cytoskeletal injury during ischemia is not confined to Z/PACs alone, but affects other structures related to the plasmalemma.

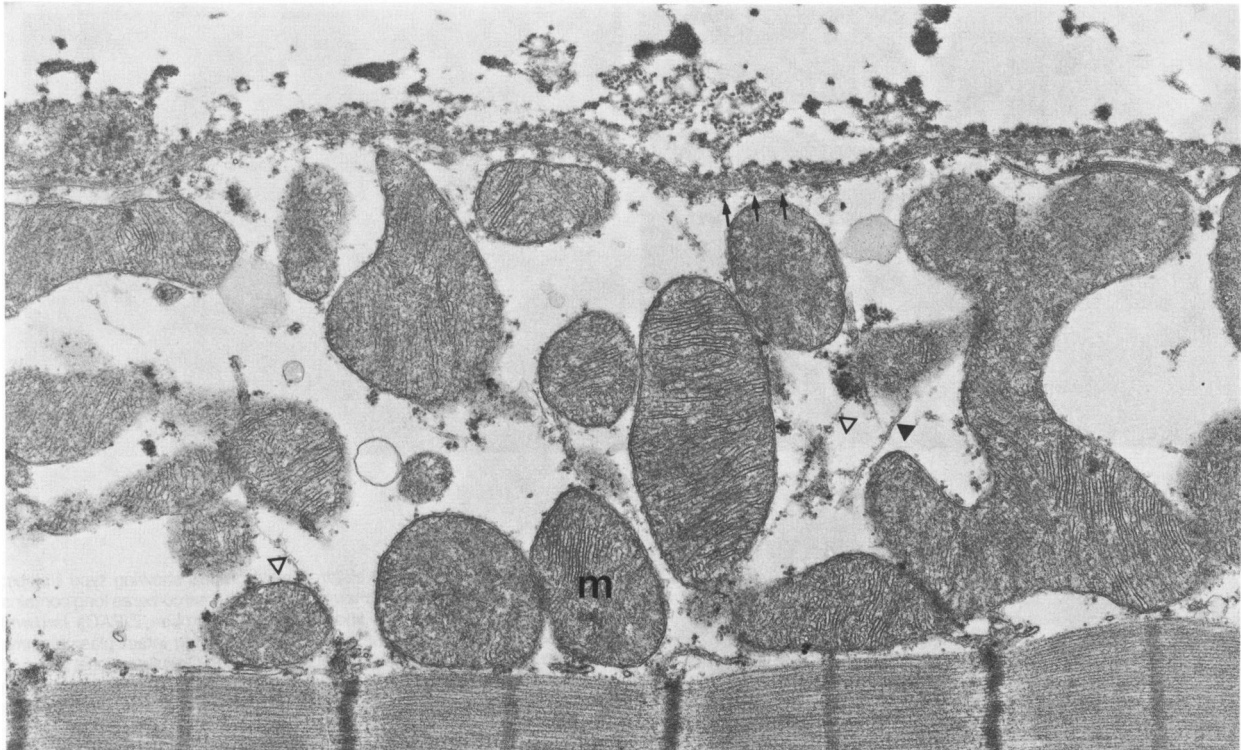


Figure 4—Transmission electron micrographs of a type I bleb in myocardium after 120 minutes of *in vitro* total ischemia. The bleb contains mitochondria and a few fragments of intermediate filaments (open arrowheads) and sarcoplasmic reticulum (solid arrowheads). The bleb roof shows the surface lamina attached to the plasmalemma, which has no major defects, and to the leptomere periodic subplasmalemmal densities (arrows). ($\times 21,000$)

Prevalence of Z/PAC Breakage

No published comparable quantitative data of ultrastructural examination of Z/PAC integrity were found. Ganote and Vander Heide⁷ recently showed that, at a light microscopic level, about half the cells of rat hearts subjected to anoxic hypotonic perfusion for 45 minutes showed bleb formation, and most cells exhibited blebs after 90 minutes. Their figures suggest that, compared with hypotonically perfused rat heart, blebs in dog heart during *in vitro* total ischemia appear later and are fewer in number. This difference may result from any of four factors: 1) differences between species in the rate of progression of ischemic injury¹⁷; 2) differences between models in the rate of ischemic metabolism^{1,10}; 3) different methods of quantitation; and 4) the absence in the present study of the amplifying effect on cell swelling of hypotonic perfusate. Nonetheless, Z/PAC breakage in the present study was focal and sparse before the onset of lethal injury, and while it remained focal, it became considerably more prevalent after the transition to lethal injury.

The term Z-band/plasmalemmal attachment complex (Z/PAC) was used to express the present understanding that this structure contains multiple components. The myofibrillar Z-band consists of the over-

lapped branched ends of “thin” (7 nm) F-actin filaments¹⁸ interlinked and complexed with α -actinin.¹⁹ Extending around and between adjacent Z-bands, and between the Z-bands of peripheral myofibers and the plasmalemma, are anchor fibers²⁰ that are composed of intermediate filaments of desmin subtype.^{21–24} Anchor fibers are attached to subplasmalemmal densities,^{23,25} which are the sites of immunolocalization of the direct or indirect actin-binding proteins vinculin and spectrin.^{6,26,27} These last two proteins may also form direct connection between the myofibrillar Z-band and the plasmalemma independent of intermediate filaments. The precise interaction of these components, and the possible existence of others, is unknown presently.

This uncertainty in the knowledge of normal structure limits to speculation the identification of the components that are the targets of ischemic injury to Z/PACs. There is experimental data showing that immunofluorescent antigenicity (at light microscopic level) of vinculin^{6,7} and α -actinin⁷ is lost during prolonged ischemia, but that desmin antigenicity⁷ shows no detectable alteration. No immunoelectron microscopic studies of these changes have been published to date. Attempts to obtain localization of these antigens in resin-embedded thin sections with commercially

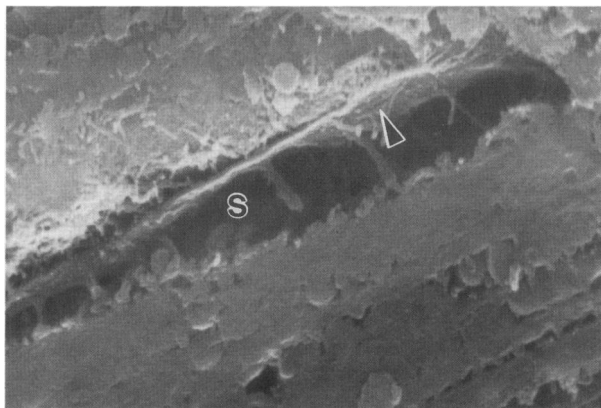


Figure 5—Scanning electron micrograph of myocardium after 120 minutes of ischemia showing a type I bleb (s). The interior surface (arrow head) of the bleb roof has a granular-nodular appearance. ($\times 7700$)

available monoclonal antibodies and protein-A gold (using the technique of Bendayan and Zollinger²⁸) have proved inconsistent, even in nonosmicated tissues embedded in LR gold resin; work in progress uses ultrathin frozen sections.

The possible mechanism of injury to any of these components of the Z/PAC is similarly speculative. One attractive hypothesis is the cleavage of components by calcium-activated proteases.^{6,7} The activation of these enzymes has been empirically shown by Tolnai and Korecky²⁹ to occur in ischemic rat hearts, even though there is an unresolved theoretical question as to whether appropriate concentrations of free Ca^{2+} and H^+ exist in the cytoplasm during ischemia to activate even the micromolar calcium-activated protease (micro-CANP) form.⁶ These enzymes are one of the few physiologic agents that will lyse desmin intermediate filaments *in vitro*,³⁰ and are probably even more active against the less stable components such as vinculin and α -actinin.^{18,19} Other hypotheses to be considered are phosphorylation of intermediate filament proteins,³⁰ and disassembly of actin complexes as a consequence of high energy phosphate (HEP) depletion. Neither of these possibilities has been experimentally demonstrated to date, although there is evidence in other cell systems for cytoskeletal lysis after depletion of ATP.^{31,32} High energy phosphate depletion is one of the key metabolic events characterizing transition from reversible to lethal myocardial ischemia,^{10,34} and the coincident time course of HEP depletion and cytoskeletal injury in the present model indicates that this association should be further investigated.

Once it is weakened or disrupted by any or all of these injurious mechanisms, the cytoskeleton no longer provides adequate protection against two physical forces occurring during progression of ischemia.

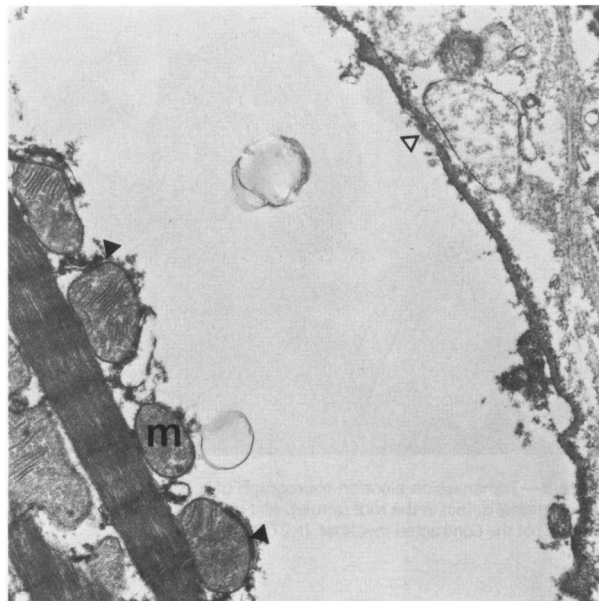


Figure 6—Transmission electron micrograph of a type II bleb present at 180 minutes of ischemia. A mitochondrion (m) containing an amorphous matrix density is evidence of irreversible injury. The subplasmalemmal network is detached from the plasmalemma and has formed an amorphous mat (black arrowheads) still attached to Z-bands of myofibrils and overlying mitochondria. The vesicular structures in the bleb space do not have a unit membrane. There are unequivocal breaks in the plasmalemma (open arrowheads). ($\times 10,000$)

First, the outwardly distensive force produced by cell swelling could “push” the plasmalemma off its attachments to underlying myofibers. This concept is supported by quantitative evidence from a previous study³⁴ that showed that myocytes could control their membrane permeability during *in vitro* total ischemia for 60–75 minutes, but thereafter inulin-diffusible space increased rapidly to reach a maximum at 200 minutes³⁴ (Figure 4). Alternatively, the onset of severe myofibrillar contracture could “pull” the myofibers

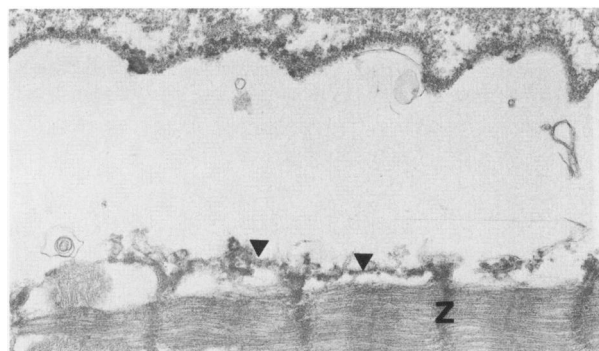


Figure 7—Transmission electron micrograph of a type II bleb after 150 minutes of ischemia. The myofibrils are in contracture and a mat of densely stained debris (arrowheads) extends over 4 sarcomeres and is attached at Z-bands (Z). The bleb roof is widely separated from the myofiber and shows only minute fragments of plasmalemma. ($\times 11,400$)

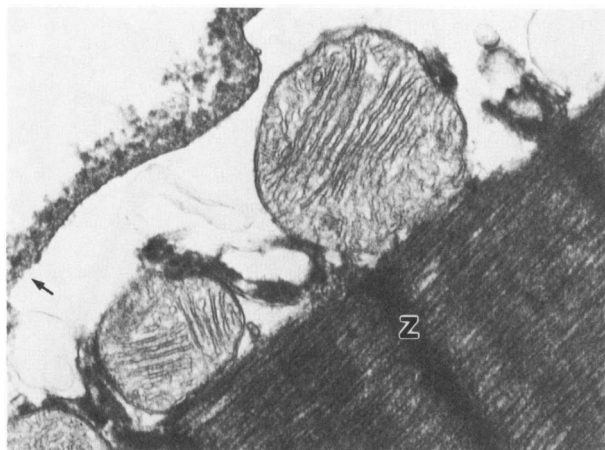


Figure 8—Transmission electron micrograph of a type II bleb showing a plasmalemmal defect in the roof (arrow), and dense material attached at Z-bands (Z) of the contracted myofiber. ($\times 27,800$)

off their membrane attachments.⁷ The ultrastructural findings of this study show that both these possibilities may occur: blebs were few before the onset of contraction or severe degrees of cell swelling (at about 120 minutes) but were numerous thereafter.

Bleb Structure

Wide variation in the form of blebs has been illustrated in previous ultrastructural studies.^{1,4,6,7} The majority of illustrated blebs can be classified as type II because they show plasmalemmal disruption, surface lamina separation, or both, and commonly show electron-dense material on the bleb floor. These appearances are closely similar to those of type II blebs seen in the present study.

Discrimination of the other predominant form (type I) described in this study was dependent on the use of aldehyde-amine fixation at 37 C.¹² The authors

have demonstrated recently¹¹ that this technique provides improved preservation of a key subplasmalemmal structure: the leptomere.³⁵⁻³⁹ This periodic array is composed of dense bars about 20 nm in diameter and up to 200 nm long that are distributed along the sarcomere with a regular 150–200 nm spacing, and are linked together by 7 nm diameter microfilaments. Type I blebs are formed by breakage of Z/PACs, but the sarcolemmal roof shows an intact plasmalemma and surface lamina, and the characteristic periodic densities of the leptomeres attached to the inner or cytoplasmic face of the plasmalemma. In type II blebs, Z/PACs are broken and the leptomeres are detached from the surface of the plasmalemma, which is frequently disrupted. The existence of type I blebs is an important finding because it demonstrates that Z/PAC breakage can precede plasmalemma disintegration, and that leptomeres may have an important role in protecting regions of plasmalemma between Z/PACs from distensive stresses such as those induced by cell swelling.

Type I blebs have a different structure from type II blebs and it is surmised that the two forms may differ in their mechanism of formation. The finding that type II blebs showed separation from the plasmalemma of subplasmalemmal leptomere arrays and surface lamina, and the retention of bleb base structures, leads to speculation that type II bleb formation is mediated at the membrane level. This could occur either by lysis of cytoskeletal linkage proteins (such as spectrin, vinculin and α -actinin) attached to (or embedded in) the plasmalemma, or by disintegration of the membrane itself. Type I blebs showed intact sarcolemmal organization, suggesting that they were formed by lysis of Z/PACs alone.

Though the possibility of a single mechanism cannot be excluded, the authors suggest that these two

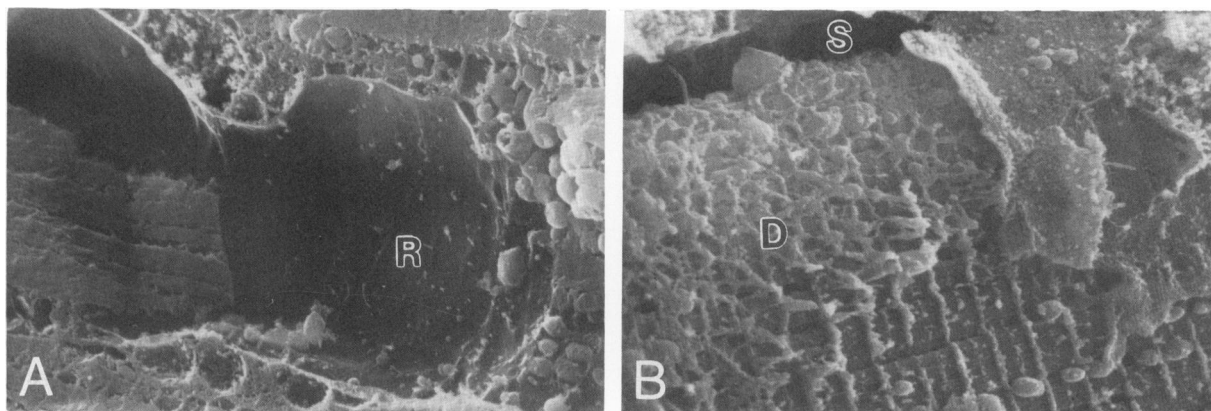


Figure 9—Scanning electron micrographs of type II blebs present at 180 minutes of ischemia showing **A**—the smooth interior surface of the bleb roof (R), and **B**—bleb space (S) and dense array of stranded material (D) adherent to the peripheral myofibers. ($\times 5500$)

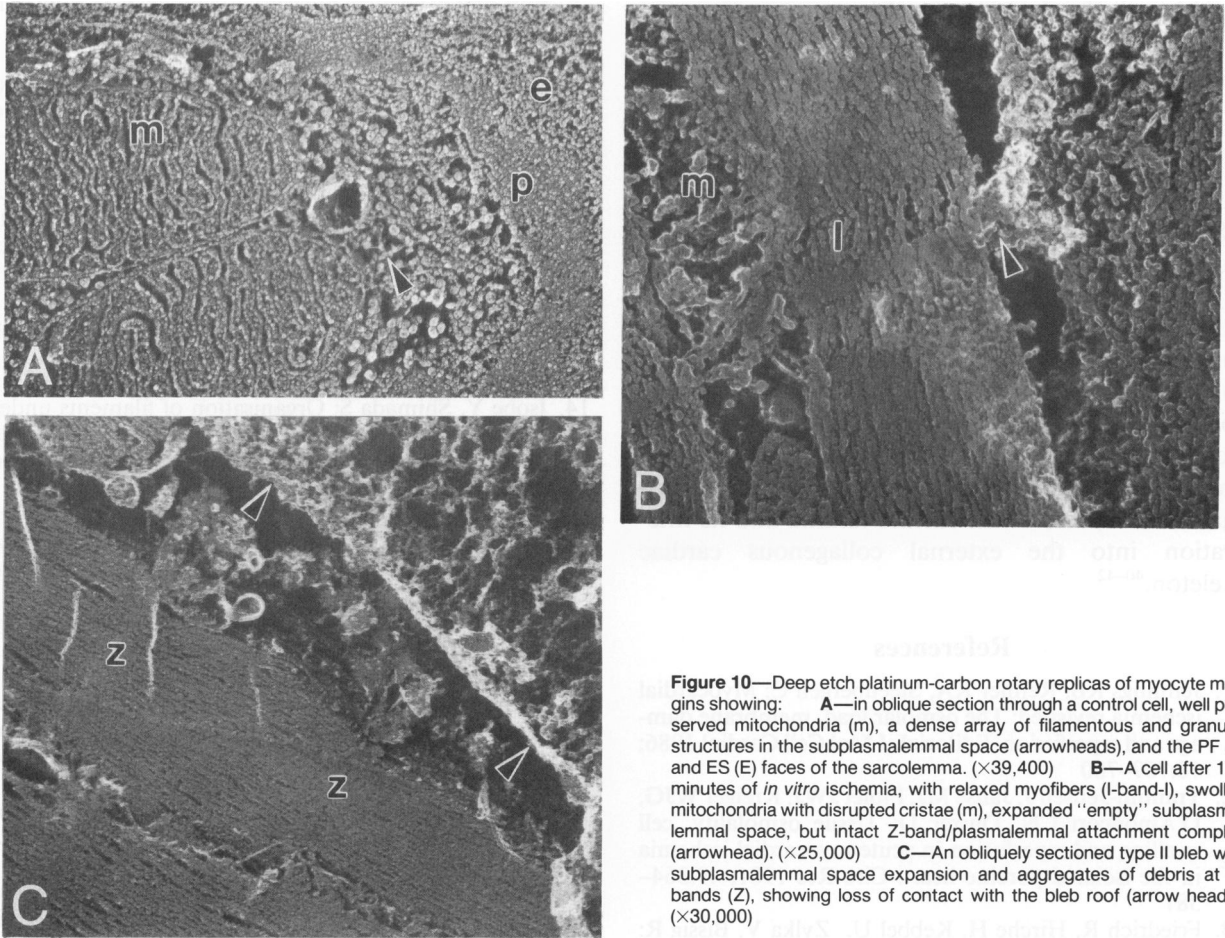


Figure 10—Deep etch platinum-carbon rotary replicas of myocyte margins showing: **A**—in oblique section through a control cell, well preserved mitochondria (m), a dense array of filamentous and granular structures in the subplasmalemmal space (arrowheads), and the PF (P) and ES (E) faces of the sarcolemma. ($\times 39,400$) **B**—A cell after 120 minutes of *in vitro* ischemia, with relaxed myofibers (I-band-I), swollen mitochondria with disrupted cristae (m), expanded “empty” subplasmalemmal space, but intact Z-band/plasmalemmal attachment complex (arrowhead). ($\times 25,000$) **C**—An obliquely sectioned type II bleb with subplasmalemmal space expansion and aggregates of debris at Z-bands (Z), showing loss of contact with the bleb roof (arrow heads). ($\times 30,000$)

types of blebs result from separate mechanisms that may act consecutively or concurrently. Such a two-step mechanism would also explain the appearance in late ischemic samples of blebs described earlier as “modified type I.” This type of bleb showed Z/PAC breakage, no bleb floor debris, but disorganised subplasmalemmal

leptomeres, a pattern consistent with an initial Z/PAC-directed insult followed by a secondary membrane-directed insult. The observation that type I blebs appeared earlier than type II blebs also suggests that the Z/PAC-directed insult may be initiated earlier in ischemia than the membrane-directed insult.

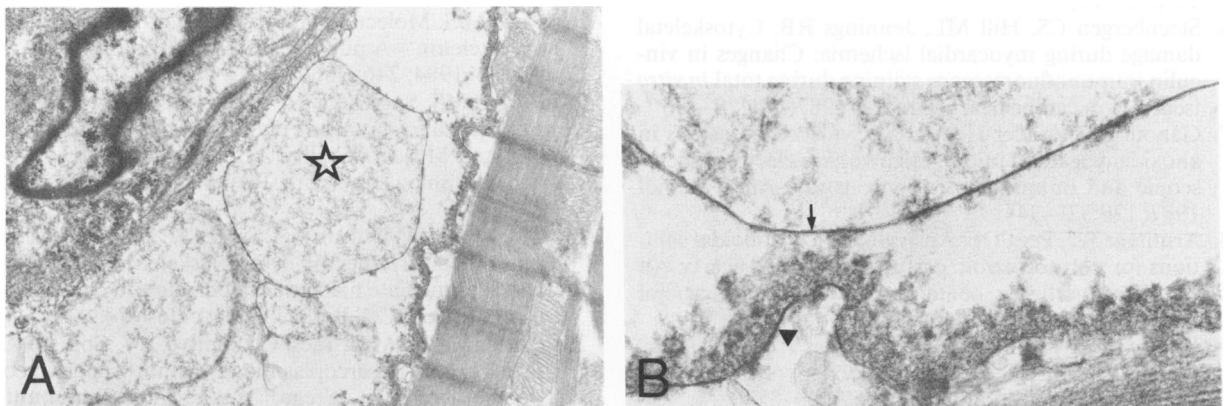


Figure 11—Transmission electron micrographs of myocardium after 180 minutes of ischemia showing **A**—type III blebs (*) in the interstitium between the myocyte and an obliquely sectioned capillary wall. ($\times 10,700$) **B**—Detail of the unit membrane of the type III bleb (arrow) and the adjacent myocyte (arrowhead). ($\times 48,000$)

Although the detachment of leptomers from the plasmalemma has a temporally and structurally close relationship to type II bleb formation, and thus to a possible membrane-directed insult, this does not allow one to infer cause and effect. It may be that loss of leptomere integrity is one of the causative steps in membrane destruction, but this remains unproven. The authors conclude, however, that any future consideration of membrane destruction during ischemic injury must examine not just the plasmalemmal-myofibrillar attachment components of the cytoskeleton, but also structures such as leptomers that attach to the plasmalemma between the relatively widely spaced Z/PACs. Further investigations might consider attachments at myofibrillar M-bands,⁶ a microfilamentous array organizing the entire subplasmalemmal space, or the surface lamina and its integration into the external collagenous cardiac skeleton.⁴⁰⁻⁴²

References

- Jennings RB, Reimer KA, Steenbergen C: Myocardial ischemia revisited: The osmolar load, membrane damage and reperfusion. Editorial. *J Mol Cell Cardiol* 1986; 18:769-780
- Tranum-Jensen J, Janse MJ, Fiolet JWJ, Kreiger WJG, D'Alnoncort CN, Durrer D: Tissue osmolality, cell swelling and reperfusion in acute myocardial ischemia in the isolated porcine heart. *Circ Res* 1981; 49:364-381
- Friedrich R, Hirche H, Kebbel U, Zylka V, Bissig R: Changes of extracellular Na⁺, K⁺, Ca²⁺, and H⁺ of ischemic myocardium in pigs. *Bas Res Cardiol* 1981; 76: 453-456
- Steenbergen CS, Hill ML, Jennings RB: Volume regulation and plasma membrane injury in aerobic, anaerobic and ischemic myocardium *in vitro*. Effects of osmotic cell swelling on plasma membrane integrity. *Circ Res* 1985; 57:864-875
- Vander Heide RS, Ganote CE: Increased myocyte fragility following anoxic injury. *J Mol Cell Cardiol* 1987; 19:1085-1103
- Steenbergen CS, Hill ML, Jennings RB: Cytoskeletal damage during myocardial ischemia: Changes in vinculin immunofluorescence staining during total *in vitro* ischemia in canine heart. *Circ Res* 1987; 60:478-486
- Ganote CE, Vander Heide RS: Cytoskeletal lesions in anoxic myocardial injury: High voltage electron microscopic and immunofluorescence study. *Am J Pathol* 1987; 129:327-344
- Armitage WJ, Pegg DE: An evaluation of colloidal solutions for normothermic perfusion of rabbit hearts: An improved perfusate containing Haemaccel. *Cryobiol* 1977; 14:428-434
- Herdson PB, Kaltenbach JP, Jennings RB: Fine structural and biochemical changes in dog myocardium during autolysis. *Am J Pathol* 1969; 57:539-557
- Jennings RB, Reimer KA, Hill ML, Mayer SE: Total ischemia in dog hearts *in vitro*. I: Comparison of high energy phosphate production, utilization and depletion, and of adenine nucleotide catabolism in total ischemia *in vitro* vs. severe ischemia *in vivo*. *Circ Res* 1981; 49:892-900
- Sage MD, Jennings RB: Subplasmalemmal leptomers in adult canine myocytes: Putative cytoskeletal function and the effect of total *in vitro* ischemia. *Lab Invest* 1988, submitted for publication
- Boyles J, Fox JEB, Phillips DR, Stenberg PE: Organization of the cytoskeleton in resting, discoid platelets: Preservation of actin filaments by a modified fixation that prevents osmium damage. *J Cell Biol* 1985; 101: 1463-1472
- Sage MD, Jennings RB: Myocyte swelling and plasmalemmal integrity during early experimental myocardial ischemia *in vivo*. *Scanning Microsc* 1988; 2:477-484
- Isobe Y, Shimada S: Organisation of filaments underneath the plasma membrane of developing chicken skeletal muscle cells *in vitro* revealed by the freeze-dry rotary replica method. *Cell Tiss Res* 1986; 244:47-56
- Nassar R, Wallace NR, Taylor I, Sommer JR: The quick freezing of single intact skeletal muscle fibers at known time intervals following electrical stimulation. *Scanning Electron Microsc* 1986; Part I:309-328
- Ganote CE, Humphrey SM: Effects of anoxic or reoxygenated reperfusion in globally ischemic, isovolumic, perfused rat hearts. *Am J Pathol* 1985; 120:129-145
- Hearse DJ, Humphrey SM, Garlick PB: Species variation in myocardial anoxic enzyme release, glucose protection and reoxygenation damage. *J Mol Cell Cardiol* 1976; 8:329-339
- Yamaguchi M, Robson RM, Stromer MH: Evidence of actin involvement in cardiac Z-lines and Z-line analogues. *J Cell Biol* 1983; 96:435-442
- Reddy MK, Rabinowitz M, Zak R: Stringent requirements for Ca²⁺ in the removal of Z-lines and α -actinin from isolated myofibrils by Ca²⁺-activated neutral proteinase. *Biochem J* 1983; 209:635-641
- Sommer JR, Jennings RB: Ultrastructure of cardiac muscle, *The Heart and Cardiovascular System*. Edited by HA Fozzard, E Haber, RB Jennings, AM Katz, HE Morgan. New York, Raven Press, 1986, pp 61-100
- Price MG, Sanger JW: Intermediate filaments in striated muscle: A review of structural studies in embryonic and adult skeletal and cardiac muscle, *Cell and Muscle Motility*, Vol 3. Edited by RM Dowben, JW Shay, New York, Plenum Press, 1983, pp 1-40
- Price MG: Molecular analysis of intermediate filament cytoskeleton—A putative load bearing structure. *Am J Physiol* 1984; 246:H566-572
- Forbes MS, Sperelakis N: The membrane systems and cytoskeletal elements of mammalian myocardial cells, *Cell and Muscle Motility*, Vol 3. Edited by RM Dowben, JW Shay, New York, Plenum Press, 1983, pp 89-155
- Tokuyasu KT, Dutton AH, Singer SJ: Immunoelectron microscopic studies of desmin (skeleton) localization and intermediate filament organization in chicken cardiac muscle. *J Cell Biol* 1983; 96:1736-1742
- Chiesi M, Ho MM, Inesi G, Somlyo AV, Somlyo AP: Primary role of sarcoplasmic reticulum in phasic contractile activation of cardiac myocytes with shunted myolemma. *J Cell Biol* 1981; 91:728-742
- Pardo JV, Siciliano JD, Craig SW: Vinculin is a component of an extensive network of myofibril-sarcolemma

- attachment regions in cardiac muscle fibers. *J Cell Biol* 1983; 97:1081–1088
27. Menold MM, Repasky EA: Heterogeneity of spectrin distribution among avian muscle fiber types. *Muscle and Nerve* 1984; 7:408–414
 28. Bendayan M, Zollinger M: Ultrastructural localization of antigenic sites on osmium-fixed tissues applying the Protein A-Gold technique. *J Histochem Cytochem* 1983; 31:101–109
 29. Tolnai S, Korecky B: Calcium dependent proteolysis and its inhibition in ischemic rat myocardium. *Can J Cardiol* 1986; 2:42–47
 30. Traub P: Post-translational modification of intermediate filament proteins, *Intermediate Filaments: A Review*. Heidelberg, Springer Verlag, 1985, pp 140–169
 31. Bershadsky AD, Gelfand VI, Svitkina TM, Tint IS: Destruction of microfilament bundles in mouse embryo fibroblasts treated with inhibitors of energy metabolism. *Exp Cell Res* 1980; 127:421–429
 32. Wang Y-L: Reorganisation of α -actinin and vinculin in living cells following ATP depletion and replenishment. *Exp Cell Res* 1986; 167:16–28
 33. Jennings RB, Hawkins HK, Lowe JE, Hill ML, Klotman S, Reimer KA: Relation between high energy phosphate and lethal injury in myocardial ischemia in the dog. *Am J Pathol* 1978; 92:187–214
 34. Jennings RB, Steenbergen C, Kinney RB, Hill ML, Reimer KA: Comparison of the effect of ischaemia and anoxia on the sarcolemma of the dog heart. *Eur Heart J* 1983; 4(Suppl H):123–127
 35. Ruska H, Edwards GA: A new cytoplasmic pattern in striated muscle fibers and its possible relation to growth. *Growth* 1957; 21:73–88
 36. Thoenes W, Ruska H: Uber "Leptomere myofibrillen" in der Herzmuskelzelle. *Z Zellforsch* 1960; 51:560–570
 37. Johnson EA, Sommer JR: A strand of cardiac muscle: Its ultrastructure and the electrophysiological implications of its geometry. *J Cell Biol* 1967; 33:103–129
 38. Karlsson U, Andersson-Cedergren E: Small leptomeric organelles in intrafusal muscle fibers of the frog as revealed by electron microscopy. *J Ultrastruct Res* 1968; 23:417–426
 39. Viragh S, Challice CE: Variations in filamentous and fibrillar organisation, and associated sarcolemmal structures, in cells of the normal mammalian heart. *J Ultrastruct Res* 1969; 28:321–334
 40. Koteliansky VE, Shirinsky VP, Gneushev GN, Chernousov MA: The role of actin-binding proteins vinculin, filamin and fibronectin in intracellular and intercellular linkages in cardiac muscle. *Adv Myocardiol* 1985; 5:215–221
 41. Caulfield JB, Borg TK: The collagen network of the heart. *Lab Invest* 1979; 40:364–372
 42. Robinson TF, Cohen-Gould L, Factor SM: Skeletal framework of mammalian heart muscle. Arrangement of inter- and pericellular connective tissue structures. *Lab Invest* 1983; 49:482–498

Acknowledgment

Scanning electron microscopy was undertaken with the permission of Dr. G. Klintworth at the Duke University Eye Center. Replicas were made in the laboratory of Dr. J. R. Sommer. The authors are grateful for his encouragement and the teaching of Ms. N. R. Wallace in this procedure. The figures were prepared by Mr. D. Graham and the script by Mrs. M. Thomas and Mrs. G. Cleary.